JOURNAL OF MATERIALS SCIENCE 17 (1982) 1713–1722

Failure loads for model adhesive joints subjected to tension, compression or torsion

A. N. GENT, O. H. YEOH*
Institute of Polymer Science, The University of Akron, Akron, Ohio 44325, USA

The Griffith fracture criterion has been applied to model adhesive joints subjected to tension, compression or torsion. Two model joints are considered: a rigid cylinder partly embedded in and bonded to an elastic cylinder (termed "rod joint" here), and an elastic cylinder inserted partway into, and bonded to, a rigid tube (termed "sleeve joint" here). Both types of joint have been constructed, using vulcanized rubber cylinders bonded to aluminium rods and sleeves. Measurements have been made of the failure loads under tension, compression and torsional loading. They were found to be in satisfactory agreement with the theoretical predictions except, in some instances, for rod joints subjected to tension or torsional loading when the failure loads were as much as three times the predicted values. This discrepancy is attributed to friction between the partially-detached rubber cylinder and the embedded rod, enhanced to a great extent by the tendency of the rubber cylinder to shrink in radius on stretching or twisting. A theoretical analysis of the effect of friction is presented. It predicts increasingly large pull-out forces or torques, as the depth of embedment increases, until frictional seizure occurs. Experimentally, frictional effects were limited by applying an internal gas pressure to the region being detached. All of the failure loads were then found to be in satisfactory agreement with the original theory, ignoring frictional effects. Thus, a simple fracture energy criterion is shown to govern the failure of adhesive joints under complex loading conditions, with or without friction acting at the interface.

1. Introduction

In general, the strength of an adhesively-bonded joint is a function of the mode of loading and the dimensions and elastic properties of the bonded components, as well as of the intrinsic strength of the interface. The objective of failure analysis of adhesive joints is to relate the breaking load to these diverse factors. One approach uses a simple energy criterion for fracture, in terms of a characteristic energy for breaking apart the interface. Originally proposed by Griffith [1] for the brittle fracture of solids, an energy criterion for fracture has been successfully applied to the separation of two adhering solids by a number of previous authors (for example [2–13]).

In applying an energy criterion to adhesive failure, it is first necessary to identify an initial point of separation, usually a flaw or point of high stress concentration at the interface between the two adhering solids. Then, failure is assumed to take place by growth of this initial debond until the joint is completely broken. An energy balance is formulated for a small growth of the debond: changes in the strain energy of the joint and the potential energy of the loading device are equated to the characteristic energy needed for debonding. This energy balance provides the required relationship between the breaking load, the properties of the two adhering solids and the dimensions of the joint. It has been applied to the debonding of

*On leave from the Rubber Research Institute of Malaysia, Kuala Lumpur, Malaysia.

0022–2461/82/061713–10$03.70/0

laminates by Kendall [10–12] and to the pull-out of embedded inextensible cords by Gent *et al.* [13].

Relationships obtained in this way for the failure load contain no adjustable parameters. Successful prediction of observed failure loads is therefore strong evidence for the validity of the proposed failure criterion and of the simplifying assumptions made in the analysis, which are, linearly elastic behaviour of the adherends and substantially homogeneous deformation of parts of each adherend. Moreover, the predicted failure loads may be used as the basis for rational design of bonded components, once the basic assumptions of the theory have been shown to hold. Furthermore, simple test methods can be developed for determining the characteristic strength of bonded interfaces from the measured failure loads of suitable model joints. The analysis of the pull-out force of cords embedded in rubber blocks [13] has been employed in this way to measure the adhesion of tyre cords to rubber [14].

Strong additional support for the basic concept of an energy criterion governing the failure of adhesive joints would be provided by successful analysis of more complex loading conditions. In the present work the analysis of the pull-out force for an embedded rigid cylindrical rod by Gent *et al.* [13] is extended to include compressive and torsional failure loads also, and applied to a reverse geometry, in which a cylindrical rubber rod is partly embedded in, and bonded to, a rigid cylindrical tube or sleeve. The first configuration, shown in Fig. 1a, is referred to here as the "rod joint", and the second, shown in Fig. 1b, as the "sleeve joint". Experiments on model joints, using a rubber vulcanizate bonded to aluminium rods and sleeves, are then described and the results compared to the predictions of the theoretical analysis. The theory is then extended to include a frictional interaction between the two surfaces, when they are pressed into close contact after debonding.

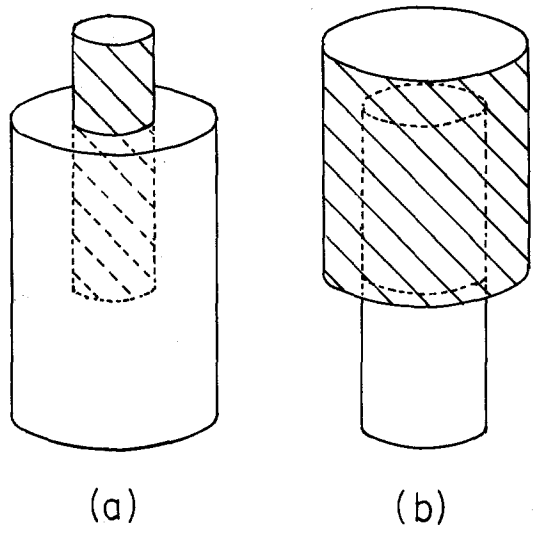

Figure 1 Sketch of model joints showing (a) rod joint and (b) sleeve joint. The rigid parts are shown shaded, the elastic parts not shaded.

2. Theoretical considerations

2.1. Rod joint

The following analysis is a generalization of that given by Gent *et al.* [13] to include compressive and torsional failure modes.

A rigid rod, radius a, is partly embedded in and bonded to a rubber cylinder of radius r. Debonding is effected by one of the following means:

(a) application of a tensile force, F (Fig. 2a),

(b) application of a torque, M (Fig. 2a),

(c) application of a compressive force, F (Fig. 2b).

Note that for the compressive experiments a hole was provided in the rubber cylinder to accommodate the displacement of the rod, as shown schematically in Fig. 2b.

Debonding is expected to initiate quite easily at the embedded end of the rod because of the high stress concentration there. Consider the situation after a small debond of length x has developed. The rubber cylinder may then be regarded as made up of three regions, i.e.,

Region A: This part is still bonded to the rod. It is assumed that the rubber in this region is unstrained.

Region B: This part, in the form of a tube of length x, is no longer bonded to the rod. It is assumed that the rubber in this region is in a state of simple extension, compression, or torsion depending on the type of loading.

Region C: The end region is assumed to be substantially in simple extension, compression or torsion; however, its exact state of deformation does not enter into consideration as long as it remains constant under a constant (failure) load. Propagation of the debond by a small amount Δx results in the growth of Region B by an amount Δx at the expense of Region A. Thus, the volume of rubber subjected to strain increases by an amount $\pi(r^2 - a^2)\Delta x$ and the total strain energy of the joint increases correspondingly. However,

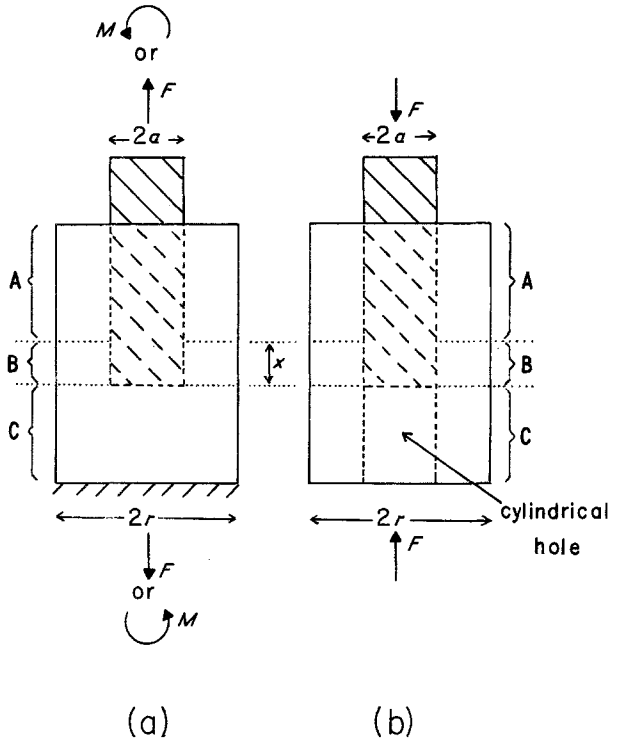

Figure 2 Rod joint in (a) tension or torsion and (b) compression (note hole to accommodate displacement of the rod). The rigid parts are shown shaded, the elastic parts not shaded.

the potential energy of the loading device decreases. The difference between the energy supplied by the loading device and the gain in strain energy is the energy available for fracture. For debond propagation, this energy must equal or exceed the energy requirement for fracture, i.e., $2\pi a\Delta x G_a$, where G_a is the characteristic energy required to fracture unit area of the adhesive interface.

The energy balance equation can be written explicitly provided the stress–strain properties of the rubber are known. For simplicity, it is first assumed that the rubber is linearly elastic with Young's modulus E and a shear modulus equal to $\frac{1}{3}E$.

For tension and compression, the energy supplied by the load F is $Fe\Delta x$ where e is the strain in Region B, given by $e = F/\pi(r^2 - a^2)E$. The increase in strain energy is $\frac{1}{2}Fe\Delta x$ or half the work done by the load. Hence for debond propagation,

$$\tfrac{1}{2}Fe\Delta x > 2\pi a\Delta x\, G_a. \qquad (1)$$

Thus the relation between G_a and the failure force F_f in tension or compression is [13]

$$G_a = \frac{F_f^2}{4\pi^2 a(r^2 - a^2)E}. \qquad (2)$$

For torsion, the energy supplied by the applied torque, M, is $M\Delta\theta$, where $\Delta\theta$ is the increase in the angle of twist resulting from a debond propagation of Δx. The increase in strain energy is $\frac{1}{2}M\Delta\theta$, and hence for debond propagation,

$$\tfrac{1}{2}M\Delta\theta > 2\pi a\Delta x\, G_a. \qquad (3)$$

But from elasticity theory, $\Delta\theta$ is given by

$$\Delta\theta = \frac{6M\Delta x}{\pi(r^4 - a^4)E}. \qquad (4)$$

Thus, the predicted relation between G_a and the failure torque M_f is

$$G_a = \frac{3M_f^2}{2\pi^2 a(r^4 - a^4)E}. \qquad (5)$$

2.2. Sleeve joint

A rubber cylinder of radius a is partly embedded within, and bonded to, a rigid sleeve (Fig. 3). Debonding is again effected by either

(a) application of a tensile force, F, or

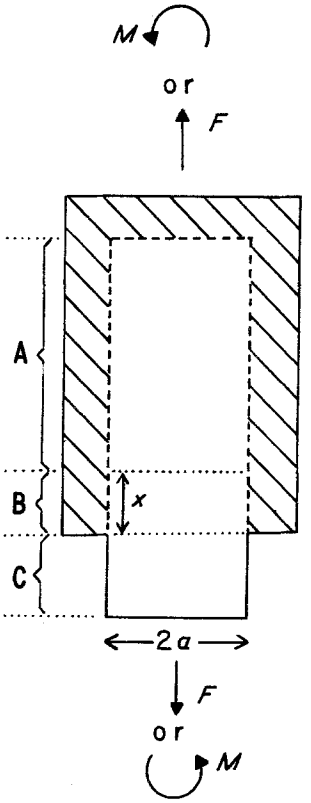

Figure 3 Sleeve joint with the rigid parts shown shaded, elastic parts not shaded.

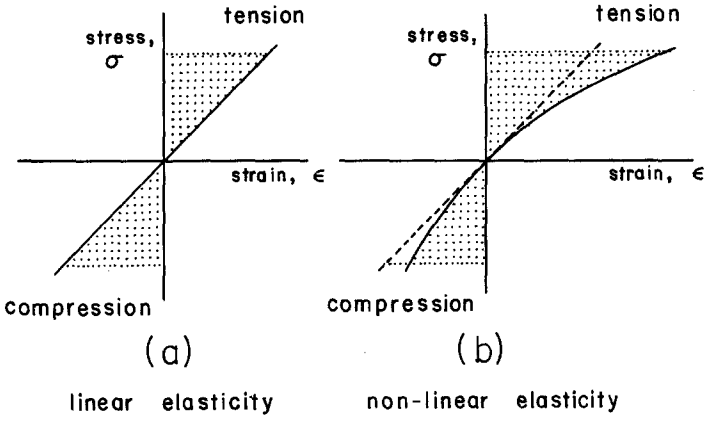

Figure 4 Schematic diagram showing energy available for debond propagation. The shaded area represents available energy.

(b) application of a torque, M.

In these cases, debonding is expected to initiate at the rim of the sleeve where the rubber cylinder enters it. After a small debond of length x has developed, the rubber cylinder may again be regarded as made up of three regions:

Region A: Where the rubber is still bonded to the sleeve and is assumed to be unstrained.

Region B: Of length x, where the rubber has become debonded and is assumed to be in a state of simple extension or torsion.

Region C: Assumed to remain in a state of simple extension or torsion under the applied load or torque.

Propagation of the debond by a small amount Δx results in the growth of Region B by Δx at the expense of Region A.

Writing the energy balance equation as before yields the results, in tension, of

$$G_a = \frac{F_f^2}{4\pi^2 a^3 E}, \tag{6}$$

and, in torsion, of

$$G_a = \frac{3M_f^2}{2\pi^2 a^5 E}. \tag{7}$$

2.3. Non-linear elasticity

The assumption of linear elasticity of rubber made in the above analysis is strictly valid only at very small strains (e.g. up to about 10% in tension or compression). If adhesive failure occurs when the rubber is subjected to higher strains, then the relations obtained will be in error by an amount dependent upon the degree of departure from linearity.

Some increase in accuracy can be obtained by assuming that the rubber obeys the statistical theory of rubber elasticity. It is known that the statistical theory gives a fairly good description of the stress–strain behaviour of well-vulcanized rubber up to moderate strains, about 50% in tension or compression [15]. Moreover, a rubber obeying the statistical theory behaves substantially linearly in torsion [15]. Thus, Equations 5 and 7 are expected to apply for relatively large torsional strains.

Equations corresponding to Equations 2 and 6 can be readily derived for a rubber obeying the statistical theory. It has been shown above that the energy available for debond propagation is the difference between the work done by the applied load and the gain in stored energy. This available energy is represented in Fig. 4 by the shaded areas. For a non-linearly elastic rubber, Fig. 4b, the available energy is underestimated in tension but overestimated in compression if linear elasticity is assumed.

The energy available for debond propagation Δx is $A\Delta x \int e \, d\sigma$, where A is the cross-sectional area of the rubber (equal to $\pi(r^2 - a^2)$ for the rod joint and πa^2 for the sleeve joint) and σ is the applied stress, equal to F/A (positive for tension and negative for compression). For a rubber obeying the statistical theory, the stress–strain relation in tension–compression can be expressed as the power series

$$e = \frac{\sigma}{E} + \left(\frac{\sigma}{E}\right)^2 + \frac{2}{3}\left(\frac{\sigma}{E}\right)^3 + \ldots\ldots \tag{8}$$

Hence the criterion for debond propagation becomes

$$A\Delta x \frac{\sigma^2}{2E}\left\{1+\frac{2}{3}\left(\frac{\sigma}{E}\right)+\frac{1}{3}\left(\frac{\sigma}{E}\right)^2+\ldots..\right\} > 2\pi a\,\Delta x\, G_a. \quad (9)$$

For the rod joint, the relation between G_a and the failure load F_f is then

$$G_a = \frac{F_f^2}{4\pi^2 a(r^2-a^2)E}\left\{1+\frac{2}{3}\left(\frac{\sigma}{E}\right)+\frac{1}{3}\left(\frac{\sigma}{E}\right)^2+\ldots..\right\} \quad (10)$$

and for the sleeve joint

$$G_a = \frac{F_f^2}{4\pi^2 a^3 E}\left\{1+\frac{2}{3}\left(\frac{\sigma}{E}\right)+\frac{1}{3}\left(\frac{\sigma}{E}\right)^2+\ldots..\right\} \quad (11)$$

2.4. Testing the theory

The above analysis has yielded theoretical relations for the fracture loads in five possible experimental configurations. The equations derived have no adjustable parameters. The characteristic failure energy, G_a, may thus be compared within this group of five experiments and it may also be determined independently in a peeling experiment. Agreement of the results from such varied experiments may be regarded as a rather stringent test of the applicability of the Griffith fracture energy criterion to the failure of adhesive joints. Furthermore, employing the same joint for experiments under different modes of loading avoids some of the experimental uncertainties associated with different sample preparations.

3. Experimental details

3.1. Materials

Rubber cylinders were prepared by a hot moulding process using the following mix formulation in parts by weight: natural rubber, 100; zinc oxide, 5; stearic acid, 2; sulphur, 2.5; N-cyclohexyl-2-benzothiazylsulphenamide, 0.6. Vulcanization was effected by heating for 45 min at 140° C. From the initial slope of the stress–strain relation of all cylindrical specimens compressed between lubricated platens, the Young's modulus, E, was found to be 1.75 MPa.

A proprietary adhesive, Chemlok 205 (supplied by Hughson Chemicals, Lord Corporation) was used for bonding the rubber to aluminium rods and sleeves during vulcanization. Although this adhesive is not normally recommended for use alone with natural rubber, it gives a bond of moderate strength, yet weak enough so that apparent interfacial failure is obtained consistently. Other adhesives, such as Chemlok 220, are normally used with natural rubber but they generally give a much stronger bond so that the rubber tears rather than detaches from the substrate.

3.2. Test-pieces

Rod and sleeve joints were prepared by vulcanizing the rubber in a transfer mould with appropriate aluminium inserts serving as the adherends. The aluminium adherends were prepared by machining them to size, polishing them with silicon carbide paper and then cleaning them with acetone before the Chemlok 205 adhesive was painted onto the curved surfaces and allowed to dry. The aluminium parts were then inserted into the mould before the rubber mix was injected and vulcanized *in situ*. For the rod joint, the rubber cylinder had a radius, r, of 12.4 mm and a length of 35 mm. The aluminium rod had an embedded length of 20 mm. Rods of various radii, in the range 0.85 to 7.5 mm, were employed but most of the experiments were carried out with rods of 5 mm radius.

For rod joints intended for testing in compression, an end-piece and rod without any adhesive was used at one end of the specimen to form the central hole and flat end. For other test-pieces, a flat aluminium end-piece painted with Chemlok 220 was used at one end. This facilitated gripping of the end of the specimen during testing and use of the stronger Chemlok 220 adhesive insured that premature failure did not occur at this end.

For the sleeve joint, the aluminium sleeve had a length of 35 or 15 mm and an internal radius ranging from 6.35 to 11.35 mm. The external radius of the rubber cylinder was the same as the internal radius of the sleeve.

To determine the adhesive fracture energy G_a independently, a peel test-piece was used, consisting of a strip of rubber, 25 mm wide, 75 mm long and 1.5 mm thick, bonded to an aluminium plate with the same Chemlok 205 adhesive.

3.3. Test procedures

All experiments were performed at room temperature, using an Instron universal testing machine. For torsion tests, a simple pulley system was used

TABLE I Results from peeling experiments

Speed (mm min^{-1})	G_a (J m^{-2})
0.5	119 ± 10
5	143 ± 12
50	173 ± 20

to convert the vertical movement of the machine cross-head to a rotation of the test-piece.

Peeling experiments were performed at a stripping angle of 90° and at speeds of 0.5, 5 and 50 mm min^{-1}. All other experiments were performed at a cross-head speed of 5 mm min^{-1}. With the pulley system used, this corresponds to about 25×10^{-3} radians min^{-1} for the torsion experiment.

4. Results and discussion

4.1. Determination of G_a

Table I gives the results obtained from peeling experiments. The characteristic energy G_a for adhesive failure was calculated from the relation

$$G_a = F_p/w \qquad (12)$$

where F_p is the steady peel force and w is the width of the adhering strip. It is seen from the results that this particular experimental system has an unexpected advantage: the bond strength is only moderately sensitive to the rate of detachment. The mean value for G_a, about 140 J m^{-2}, is taken here as representative of the interfacial bond strength at moderate rates of detachment and at ambient temperatures.

4.2. Sleeve joint

The theory developed earlier predicts that the failure force or failure torque will be independent of the length of the joint. This means that a constant failure force or torque is to be expected. This is observed in practice with the sleeve joint. Once failure has been initiated, it continues at constant force or torque.

The results obtained for the failure forces and torques with the sleeve joint under tension or torsion are summarized in Table II. Values of G_a have been calculated from them using Equations 7 and 11.

It is seen from Table II that the values of G_a obtained in this way, ranging from 104 to 180 J m^{-2}, are in fairly good agreement with each other and with the value obtained from the peel experiments (about 140 J m^{-2}). Considering the very different deformations applied to the joints and the fact that the equations used to calculate G_a have no adjustable parameters and rather strong and different dependences on the radius a of the specimen, this agreement is regarded as quite satisfactory. However, there is some indication that larger values of G_a are obtained with specimens of larger radius. This may be due to the relatively small length of the bonded part of the specimens in these cases. One assumption of the theoretical analysis, that the bonded part of the specimen is effectively unstrained, will cease to hold when the radius of the cylinder becomes comparable in size to the length of the bonded part.

4.3. Rod joint

The failure of a rod joint was found to take place quite differently in tension and in torsion, than in compression. Experiments in compression with an embedded aluminium rod of 5 mm radius gave values for the failure force of 94 ± 11 N and hence a value for the effective fracture energy G_a of 184 ± 39 J m^{-2}, in reasonably good agreement with values obtained previously. However, in both tension and torsion, no well-defined failure load was observed. Instead, the tensile force or torque increased continuously during the experiment until catastrophic failure took place. Examination of the recorded plots of load against time often showed a discontinuity at loads less than the final fracture load, when bond failure may have been initiated, but this point was not well-defined and much larger loads were required to cause fracture of the joint. The final breaking force or torque has been taken here as the failure load.

TABLE II Results for sleeve joints

Radius (mm)	Length (mm)	Tension		Torsion	
		F_f (N)	G_a (J m^{-2})	M_f (Nm)	G_a (J m^{-2})
6.35	15	40 ± 2	104 ± 11	0.112 ± 0.007	106 ± 14
6.35	35	42 ± 2	112 ± 12	0.112 ± 0.005	106 ± 9
9.55	35	77 ± 2	109 ± 5	0.343 ± 0.005	129 ± 4
11.35	35	113 ± 11	141 ± 28	0.626 ± 0.013	180 ± 8

TABLE III Results for rod joints (rod radius 5 mm)

Mode of deformation	Failure load (N)	G_a (J m^{-2})
Tension	250 ± 49	1880 ± 810
Compression	94 ± 11	184 ± 39
Torsion	1.18 ± 0.20*	1060 ± 380

*In units of Nm.

Values of the failure loads in tension and torsion are given in Table III for a rod joint having an embedded rod of 5 mm radius. Values of the apparent fracture energy G_a calculated from the observed failure loads are also given in Table III. They are seen to be much greater than before. Measurements with embedded rods of different radii are reported in Table IV. They reveal that the apparent fracture energy increases as the radius of the embedded rod increases. Only for rods of relatively small radius are the calculated fracture energies comparable to those obtained previously; otherwise, they are considerably larger. Clearly, a significant factor has been omitted from the theoretical analysis for the cases of a rod joint subjected to tension or torsional loading, and this factor becomes increasingly important as the radius of the embedded rod is increased. It is attributed to frictional effects, for the following reasons.

Referring to the sketch in Fig. 2a, it has been assumed that a Region B of debond develops during tension or torsional failure of a rod joint. This region is essentially a rubber tube, placed in tension or torsion by the applied forces after debonding. Now, on stretching a rubber tube, the radius tends to undergo Poissonian contraction, and there is a similar tendency for the radius to shrink when a tube is subjected to torsion [16, 17]. Thus, for a rod joint under tension or torsion loading the debonded tube will tend to grip the embedded rod tightly and increase any frictional forces acting at the interface. On the other hand, for a rod joint under compressive loads, Fig. 2b, the rubber tube formed by debonding will tend to spread outwards away from the embedded rod, so that frictional effects should be absent in this case. Similarly, for a sleeve joint subjected to tension or torsional loads, contraction of the rubber cylinder after debonding will cause it to move away from the surrounding rigid sleeve and friction effects will again be absent.

Thus, the two test configurations which give rise to anomalously high failure loads and hence effective fracture energies, are also those for which the rubber section is pressed into close contact with the rigid inclusion after debonding. An approximate theoretical treatment of the corresponding frictional contribution to the work of detachment is given in the next section of this paper, and some experiments designed to minimize frictional effects during tension and torsional fracture of rod joints are described in the following section.

5. Frictional contribution to the fracture energy for a rod joint subjected to tension or torsion

5.1. Theoretical considerations

A rather approximate estimate of the contribution to the failure loads from friction can be made, as follows. It is assumed that the frictional stress, τ, is uniform over the debonded region (B in Fig. 2a) and given by

$$\tau = \mu P, \tag{13}$$

where μ is the coefficient of friction and P is the normal pressure acting on the embedded rod. The frictional force resisting pull-out, acting over the Region B, is therefore given by $2\pi ax\mu P$ and the additional work required to cause an incremental debond of length Δx is $2\pi ax\mu Pe\Delta x$. Thus, the energy balance equation now becomes:

$$F^2/2\pi\,(r^2 - a^2)E > 2\pi aG_a + 2\pi ax\mu Pe. \tag{14}$$

The tensile strain, e, of the debonded rubber is

TABLE IV Results for rod joints (rods of different radii)

Rod radius, a (mm)	Tension		Torsion	
	F_f (N)	G_a (J m^{-2})	M_f (Nm)	G_a (J m^{-2})
0.85	60 ± 5	430 ± 80	–	–
1.2	79 ± 12	540 ± 170	–	–
2.5	179 ± 13	1470 ± 230	0.38 ± 0.08	220 ± 84
5.0	250 ± 49	1880 ± 810	1.18 ± 0.20	1060 ± 380
7.5	346 ± 31	3770 ± 890	> 2	> 2000

given by $F/\pi(r^2 - a^2)E$ and the pressure, P, is given, for small strains, by the relation [16, 17]:

$$P = (r^2 - a^2)Ee/3r^2. \quad (15)$$

On substituting for P and e in terms of the applied load, F, the pull-out force in the presence of friction is obtained in the form

$$F^2 = \frac{4\pi^2 a(r^2 - a^2)E G_a}{[1 - (4a\mu x/3r^2)]}. \quad (16)$$

It is clear that the pull-out force is increased by friction and that it becomes larger as debonding continues, i.e., as x increases, so that the force required to propagate the debond rises continuously, rather than remaining constant. This is in accord with observation. Indeed, the pull-out force is predicted to become infinitely large when the debonded length x reaches a critical value, x_c, given by

$$x_c = 3r^2/4a\mu. \quad (17)$$

Thus, for thin-walled rubber tubes, a rod embedded to a depth much greater than its radius will be gripped by friction to such a degree that, even in the absence of bonding, pull-out will be impossible. The critical embedment depth x_c for thick-walled tubes is predicted to be considerably larger, however.

Previous studies of the pull-out force for embedded cords dealt with relatively small-radius cords [13]. In such cases, frictional contributions to the observed failure loads would be expected to be small, unless the cords were embedded to great depths, approaching x_c.

Similar considerations apply to the torsional failure of a rod joint in the presence of friction. In this case the additional work required to cause an incremental debond of length Δx is $2\pi a^2 \mu P\theta \Delta x$, where $\theta = 6Mx/\pi(r^4 - a^4)E$.

The energy balance equation then becomes

$$3M^2/\pi(r^4 - a^4)E > 2\pi a G_a + 2\pi a^2 \mu P\theta. \quad (18)$$

On substituting for θ in terms of M, and for pressure, P, from the relation [16, 17],

$$P = E(r^2 - a^2)\theta^2/6x^2, \quad (19)$$

the failure torque, M, in the presence of friction is given by the following implicit relation:

$$M^2 = \frac{2}{3}\pi^2 a(r^4 - a^4)E G_a + \frac{24a^2\mu(r^2 - a^2)xM^3}{\pi(r^4 - a^4)^2 E}. \quad (20)$$

At a critical value of the debond length x, denoted x_c, the failure torque is entirely accounted for by friction, even in the absence of any bonding ($G_a = 0$). The corresponding torque, denoted M_c, is the maximum that could give rise to further debonding. If the applied torque exceeds this value, then the work expended in frictional sliding would exceed that available so that no motion is possible. The critical torque is given by

$$M_c = \pi a^4 \left(\frac{r^2}{a^2} + 1\right)^2 \left(\frac{r^2}{a^2} - 1\right) E/24\mu x \quad (21)$$

and the corresponding angle of rotation, θ_c, by

$$\theta_c = \left(\frac{r^2}{a^2} + 1\right)/4\mu. \quad (22)$$

The above theoretical considerations reveal that frictional effects will become important, and eventually dominant, for the rod joint when the rod diameter becomes comparable to the wall thickness of the rubber tube surrounding it, and when the depth of embedment is sufficiently large. Under these circumstances frictional seizure is predicted to occur. (The same principle is employed in Chinese finger cuffs: extensible tubes which grip the fingers more firmly the harder one tries to pull them out.) In the following section, experiments are described that were designed to minimize frictional effects in rod joints, and for which the original theoretical treatment, neglecting friction, should hold.

5.2. Use of internal gas pressure to minimize friction in rod joints

A small hole was drilled along the axis of the embedded aluminium rod to permit the application of nitrogen gas under pressure to the interface during a debonding experiment. This pressure was then maintained at a constant level during the application of tension or torsional loads. Failure loads were determined in this way at various values of applied internal pressure for specimens with an embedded rod of 5 mm radius. The results are shown graphically in Figs 5 and 6.

As would be expected when an internal gas pressure is applied, tending to hold the debonded rubber away from the embedded rod, the measured failure loads were much smaller than before. They fell rapidly as the internal pressure was increased from zero up to a pressure of about 100 kPa. Above this pressure, further increases in pressure

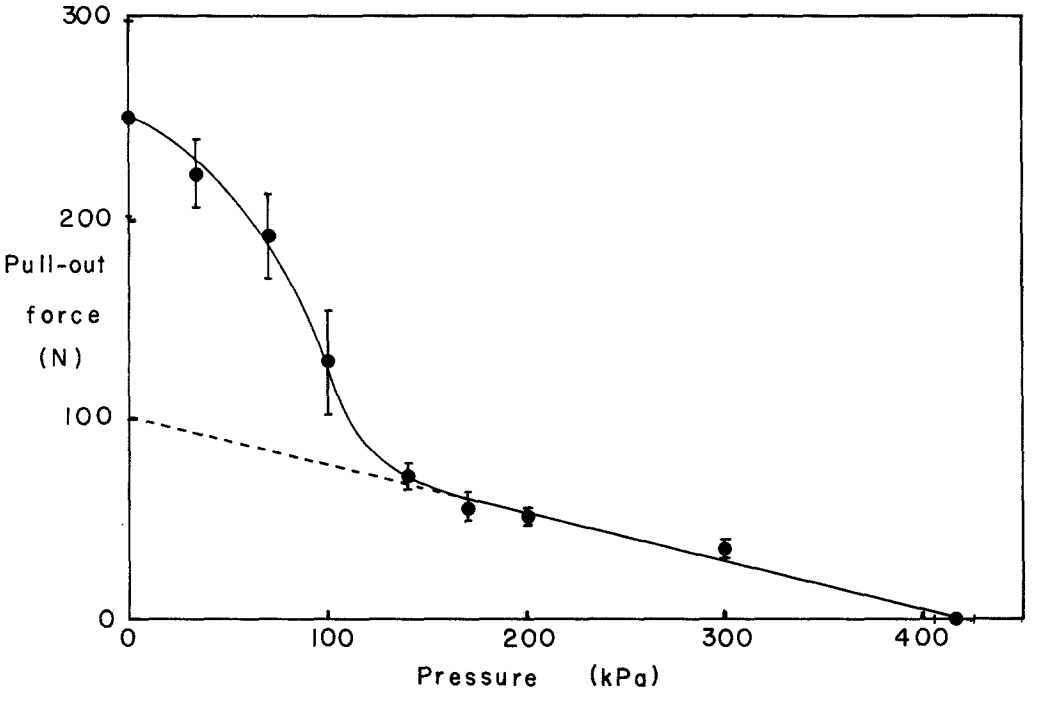

Figure 5 Dependence of pull-out force on internal pressure.

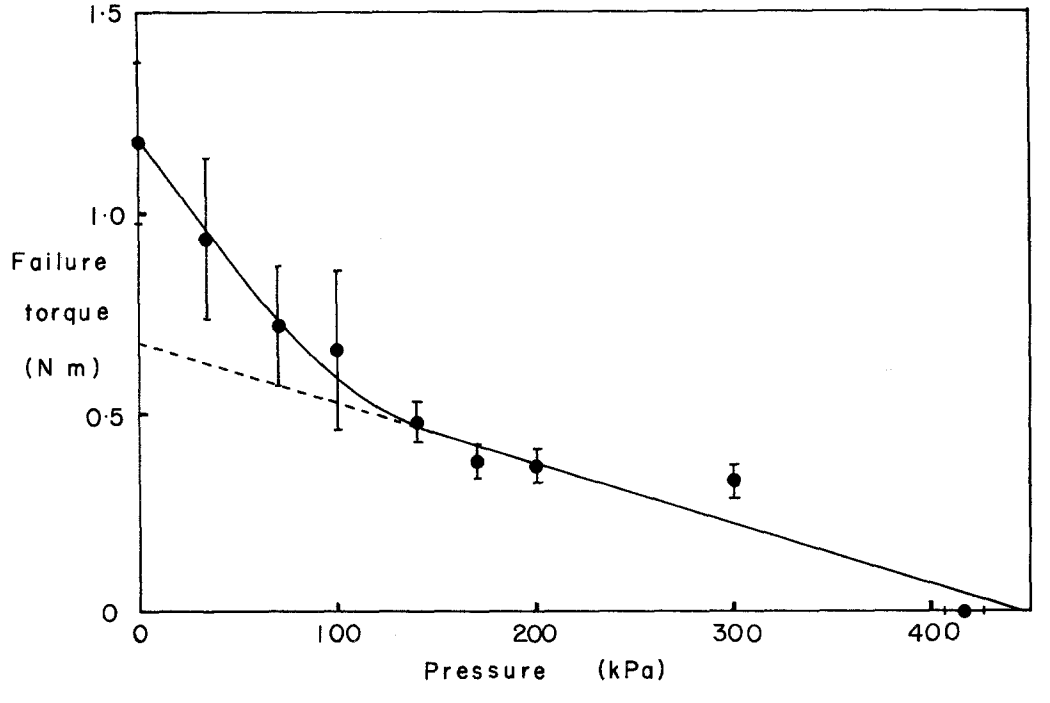

Figure 6 Dependence of failure torque on internal pressure.

had a smaller effect. Eventually, at a pressure of about 400 kPa the bond failed under the action of the gas pressure alone, without any additional load being applied.

It is assumed that the initial rapid fall in failure force or failure torque with applied pressure is due to a concurrent reduction in friction, and at the critical pressure, about 100 kPa, it is assumed that frictional effects have been virtually overcome. Slow further reductions in failure loads with further increases in gas pressure are attributed to a direct contribution to the strain energy employed in debonding from the applied pressure itself.

By extrapolating the relations observed at pressures greater than about 100 kPa, when frictional effects are assumed to be absent, back to zero pressure, as shown by the broken lines in Figs 5 and 6, values for the failure loads in the absence of friction were estimated. The values obtained in this way were a pull-out force of 100N and a failure torque of 0.68 Nm, corresponding to values of the fracture energy, G_a, of 250 and 350 J m^{-2}, respectively. These values are in approximate agreement with those obtained previously from compression experiments on rod joints, and from tension and torsion experiments on sleeve joints, indicating that the applied pressure had, indeed, eliminated the frictional contribution to the work of fracture.

6. Conclusions

The applicability of the Griffith fracture criterion to the failure of adhesive bonds has been subjected to a severe test. Two model joints have been examined under tension, compression and torsional loading and the measured failure loads compared to the theoretically-predicted values. Satisfactory agreement was obtained in all cases, except where frictional effects are significant; i.e., for a rod joint subjected to tension or torsion. When the theory is amended to take into account friction between the debonded surfaces, enhanced by the pressure generated indirectly by the applied load, then the observed increase in failure loads for rod joints is fully accounted for. Indeed, frictional seizure is predicted to occur for deeply embedded rods. Even in the absence of bonding, the load to pull out or twist free such rods is predicted to be infinitely large, due to the self-reinforcing nature of the frictional resistance.

Acknowledgements

This work was supported in part by a research contract from General Dynamics Corporation and in part by a grant from the Office of Naval Research (Number N00014-76-C-0408).

References

1. A. A. GRIFFITH, *Phil. Trans. Roy. Soc. (Lond.)* **221** (1920) 163.
2. R. S. RIVLIN, *Paint Technol.* 9 (1944) 215.
3. B. V. DERYAGIN and N. A. KROTOVA, *Dokl. Akad. Nauk. SSSR* **61** (1948) 849.
4. E. J. RIPLING, S. MOSTOVOY and R. L. PATRICK, *Mater. Res. Stand.* 4 (1963) 129.
5. B. M. MALYSHEV and R. L. SALGANIK, *Int. J. Fracture Mech.* 1 (1965) 114.
6. M. L. WILLIAMS, Proceedings of the 5th U.S. National Congress on Applied Mechanics, Minneapolis, June, 1966 (American Society of Mechanical Engineers, New York, 1966) pp. 451–464.
7. A. N. GENT and A. J. KINLOCH, *J. Polymer Sci. A-2* 9 (1971) 659.
8. P. B. LINDLEY, *J. Inst. Rubber Industry* 5 (1971) 243.
9. W. D. BASCOM, R. L. COTTINGTON, R. L. JONES and P. PEYSER, *J. Appl. Polymer Sci.* **19** (1975) 2545.
10. K. KENDALL, *J. Phys. D: Appl. Phys.* **4** (1971) 1186.
11. *Idem, ibid.* 8 (1975) 512.
12. *Idem, J. Mater. Sci.* **11** (1976) 638.
13. A. N. GENT, G. S. FIELDING-RUSSELL, D. I. LIVINGSTON and D. W. NICHOLSON, *ibid.* **16** (1981) 949.
14. G. S. FIELDING-RUSSELL, D. W. NICHOLSON and D. I. LIVINGSTON, in "Tire Reinforcement and Tire Performance", ASTM STP 694, edited by R. A. Fleming and D. I. Livingston (American Society for Testing and Materials, Philadelphia, 1979) pp. 153–162.
15. L. R. G. TRELOAR, "The Physics of Rubber Elasticity" 3rd edition (Clarendon Press, Oxford, 1975).
16. R. S. RIVLIN, *Phil. Trans. Roy. Soc. (Lond.)* **A242** (1949) 173.
17. A. N. GENT and R. S. RIVLIN, *Proc. Phys. Soc. (Lond.)* **65B** (1952) 487.

Received 28 September
and accepted 9 November 1981